Materials and Design 62 (2014) 367–374

Contents lists available at ScienceDirect

Materials and Design

journal homepage: www.elsevier.com/locate/matdes

Solid particle erosion behavior of carbidic austempered ductile iron modified by nanoscale ceria particles

Xiaoguang Sun [a,b], You Wang [a,*], D.Y. Li [a,b], Chaohui Wang [a], Xuewei Li [a], Zhiwei Zou [a]

[a] Department of Materials Science, Harbin Institute of Technology, Harbin 150001, China
[b] Department of Chemical and Materials Engineering, University of Alberta, Edmonton, Alberta T6G 2V4, Canada

ARTICLE INFO

Article history:
Received 2 April 2014
Accepted 20 May 2014
Available online 28 May 2014

Keywords:
Cast iron
Erosive wear
Impact angle
Microstructure

ABSTRACT

In this study, the solid-particle erosion behavior of carbidic austempered ductile iron (CADI) containing different amounts of ceria nanoparticles was investigated. Attempt was made to correlate the erosion resistance of the material to its microstructure and mechanical properties. It was demonstrated that the erosion resistance of CADI was improved by adding ceria nanoparticles. The maximum erosion rate of unmodified CADI occurred at the impact angle of 60–75°, which slightly shifted to lower angles when ceria nanoparticles were added, corresponding to more ductile characteristic. During erosion tests, the retained austenite in CADI partially transformed to martensite although the transformation was suppressed by the addition of ceria nanoparticles. The ceria-modified CADI showed a considerably increased erosion resistance at various impact angles.

1. Introduction

Carbidic austempered ductile iron (CADI) has attracted increasing attention as a promising engineering material because of its high strength, relatively low cost, excellent castability and machinability [1–3]. As a new member of ductile iron family, it shows a superior abrasion resistance, compared to austempered ductile iron (ADI), due to the incorporation of an extra carbide phase into the matrix. However, the presence of the coarse carbides endows the CADI with lowered toughness and less resistance to cleavage fracture, which limits its applications [4].

As a promising wear-resistant material, CADI is expected to resist different wearing conditions, such as abrasion and erosion. In particular, its resistance to solid-particle erosion should be well evaluated, since it has been used for components in mechanical systems such as automatic molding machines, air pressure pumps and gas delivery pipes. However, studies on CADI are more focused on its abrasive wear behavior [3,5–7]. No information on erosion of CADI has been reported, although the erosion behavior of ductile irons has been extensively investigated [8–10]. Even for ductile irons, results reported in the literature are not always consistent. For instance, Hung et al. [9] observed that the angle of maximum erosion rate varied with the content of retained austenite, ranging from ~35° to ~45° for the ADI having retained austenite from 17 vol.% to 2 vol.%. Chang et al. [8] reported a single erosion rate peak appearing at 45° for ADI. However, Grilec et al. [11] observed that the maximum erosion of ductile iron occurred at 75° and ADI showed double peaks of erosion loss with a minimum at 60°. Due to the incorporation of the carbides, the erosion behavior of CADI is expected to be different from that of other ductile irons including ADI. Thus, further investigation is needed in order to better understand the erosion behavior of CADI.

In this study, the erosion behavior of CADI at different impingement angles and its evolution with accumulated erodent particles were investigated. Effects of added ceria nanoparticles on microstructure and mechanical properties of the material were analyzed and correlated to the corresponding erosion behavior.

2. Experimental details

A base ductile iron, consisting of 3.5C, 2.85Si, 0.35Mn, 0.75Cr, 0.65Cu, 0.03P, 0.025S, 0.04Mg, and balance Fe (wt%), used for making CADI samples was melted in a medium frequency induction furnace. FeSiMg9 and FeSi75 were used as nodulizer and inoculant, respectively. Different amounts (0, 0.03 wt%, 0.06 wt% and 0.09 wt%) of ceria nanoparticles in diameter of ~10 nm were respectively added to the melt prior to casting. The castings were initially austenitized at 900 °C for 60 min to achieve a uniform matrix of austenite and rapidly cooled to an austempering temperature of 280 °C for 120 min in a salt bath furnace for the formation of ausferrite. The castings were then cooled to room temperature in air.

* Corresponding author. Tel.: +86 451 86402752.
E-mail address: wangyou@hit.edu.cn (Y. Wang).

http://dx.doi.org/10.1016/j.matdes.2014.05.042
0261-3069/

Phases in the CADI were analyzed using a Rikagu X-ray diffractometer with Cu Kα radiation. The content of retained austenite was determined based on YB/T 5338-2006 standard. Intensities of {200}, {220} and {311} peaks of austenite and {200}, {211} peaks of ferrite were used for the determination [12]. A scanning electron microscope (SEM, TESCAN VEGA3 EasyProbe) was used to observe morphologies of surfaces and subsurface layers of the eroded specimens.

Erosion tests were performed to evaluate the resistance of the specimens to erosion at room temperature using an air-jet sand blasting apparatus, which has been described in detail in a previous publication [13]. The velocity of the erodent particles was estimated in the range of 45–50 m/s. Nearly round silica sand (U.S. Silica Company) with size ranging from 212 to 270 μm was used as the erodent particle. Properties of the silica sand are given in Table 1. The erosion tests were performed at various impingement angles (15°, 30°, 45°, 60°, 75°, 90°). The erosion rate was expressed as the volume loss (mm^3) caused by a unit mass of erodent particles (g). Each reported value is an average of seven measurements. The erosion resistance is represented as the reciprocal of the erosion rate.

Hardness was measured with Brinell tester. Impact toughness was evaluated according to the ASTM: E23 standard using an Amsler pendulum with an initial energy of 300 J. Unnotched samples with dimensions of 5 mm * 5 mm * 55 mm were employed.

3. Results and discussion

3.1. Erosion rate

The erosion rate of materials is affected by the impact angle. Steady-state erosion rates of CADI containing different amounts of nano-ceria are plotted against the impact angles, as shown in Fig. 1. It was observed that the erosion rates of the nano-ceria modified CADI are lower than that of the unmodified CADI at all impact angles, indicating that the ceria nanoparticles play a positive role in enhancing the erosion resistance of CADI. The unmodified CADI showed a peak erosion rate at ~75°. While the maximum erosion rate of the nano-ceria modified CADI occurred in the range of 60°, implying that the nano-ceria added CADIs are tougher than the unmodified one. In general, the maximum erosion rate appears at a low angle (15–30°) for ductile materials and at a high angle (~90°) for brittle materials [14]. And the angle corresponding to the maximum erosion rate lowers with increasing toughness and ductility.

Fig. 2 shows the changes and corresponding increments of erosion resistance with the content of nano-ceria at different impact angles. One may see that the positive effect of nano-ceria on erosion resistance exists in the entire range of impact angle. At low impact angles, the sample having 0.03% nano-ceria showed the maximum erosion resistance. With an increase in the impact angle, the peak erosion resistance belonged to the sample having 0.09% nano-ceria. The increment of erosion resistance is high at ultra-low or ultra-high impact angle. At interim angles, the increments are relatively small.

Table 1
Typical properties of the silica sand for erosion test.

Property	Value
AFS grain fineness	50
Grain shape	Rounded
Hardness (Mohs/HV)	7/1420 ± 50
Melting point (Degrees F)	3100
Mineral	Quartz
Moisture content (%)	<0.05
pH	7
Specific gravity	2.65

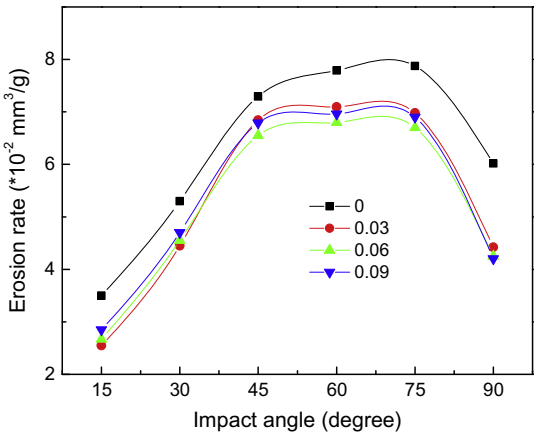

Fig. 1. Solid-particle erosion rates of nano-ceria modified CADI at various impingement angles.

Fig. 3 shows the erosion rates of CADI with different amounts of nano-ceria as a function of cumulative weight of erodent particles at impact angle of 30°, 60° and 90°. As shown, the erosion rates increased gradually from a low value to a steady one for all samples. Such a variation with the amount of erodent particles was reported to be an incubation period followed by an acceleration stage before reaching a saturated state [15]. An incubation period exists because some degree of work hardening is required before material removal during erosion. Similar trend was also observed in other ductile irons [16]. The incubation period is shortened with increasing impact angle. Because the kinetic energy of the erodent particles that could be normally exerted on the surface and used to induce plastic deformation increased with angle, it needed fewer particles to reach steady erosion.

3.2. Erosion induced phase transformation

The erosion behavior is largely dependent on the microstructure and its variation during erosion. XRD patterns of CADI before and after the erosion test are illustrated in Fig. 4. As is shown, all samples were composed of graphite, M_3C carbide, ferrite and retained austenite. The content of carbide initially increased and then decreased with the addition of ceria according to the variation in the peak intensity at 49.11° (Fig. 4a). As was reported [17], the volume fractions of carbide in the ceria-modified CADI were 11%, 15%, 14.2% and 7%, corresponding to 0%, 0.03%, 0.06% and 0.09% of nano-ceria, respectively. The austenite (111) peak at 43.278° is visible for all samples. After the erosion tests, this peak was declined evidently (Fig. 4b and c). While peaks of martensite (211) at 81.941° and (200) at 65.519° showed up, indicating the formation of martensite during erosion. The occurrence of martensite resulted from a phase transformation from retained austenite induced by external stress, similar to that inducted in ADI [18]. The retained austenite could also transform to ε-carbide for ADI during erosion process [19], which was however not observed in CADI.

Although it is difficult to accurately determine the amounts of strain-induced martensite because of the overlap between peaks of acicular ferrite and martensite [20], comparing the content of retained austenite before and after erosion tests may provide relevant information. As shown in Fig. 5, the erosion test resulted in reduced content of retained austenite and such reduction was larger when the sample was eroded at 90°, compared to that at 30°. This demonstrates that higher-angle impingement promoted the